Electronic Supporting Information (ESI) for

One-pot cation exchange synthesis of 1D porous CdS/ZnO heterostructures for visible-light-driven H_2 evolution

Xiaoxin Zou,[a,‡] Pei-Pei Wang,[a,‡] Chun-Guang Li,[a] Jun Zhao,[a] De-Jun Wang,[a,d] Tewodros Asefa,[b,c,*]

Guo-Dong Li[a,*]

[a] *State Key Laboratory of Inorganic Synthesis and Preparative Chemistry, College of Chemistry, Jilin University, Changchun 130012, China*

[b] Department of Chemistry and Chemical Biology, Rutgers, The State University of New Jersey, Piscataway, NJ 08854, USA

[c] Department of Chemical and Biochemical Engineering, Rutgers, The State University of New Jersey, Piscataway, NJ 08854, USA

[d] *Department of Chemistry, Tsinghua University, Beijing 100084, China*

* To whom correspondence should be addressed (T.A.: tasefa@rci.rutgers.edu; G.-D.L. lgd@jlu.edu.cn)

‡ Xiaoxin Zou and Pei-Pei Wang contributed equally to this work.

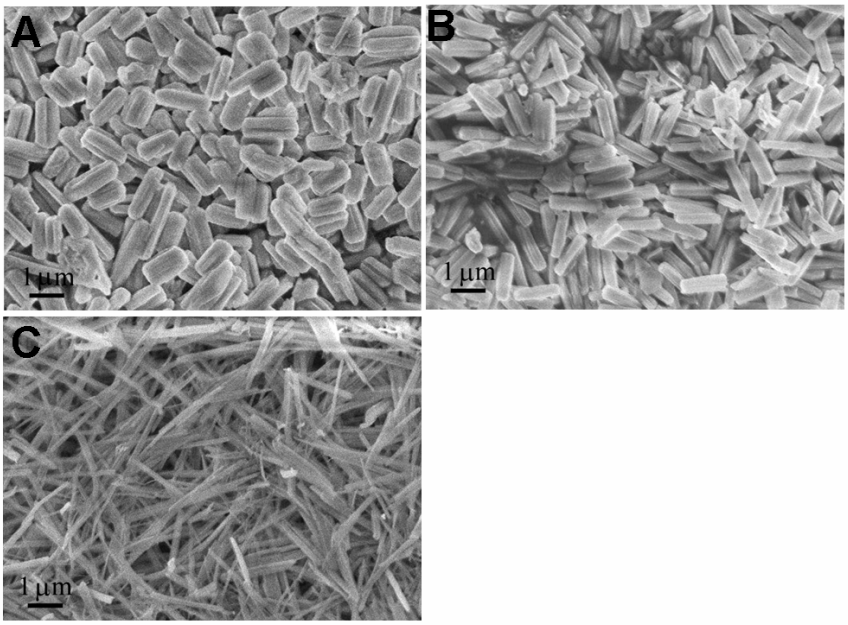

Figure S1. SEM images of (A) ZnS/CHA-1, (B) ZnS/CHA-2, and (C) ZnS/CHA-3.

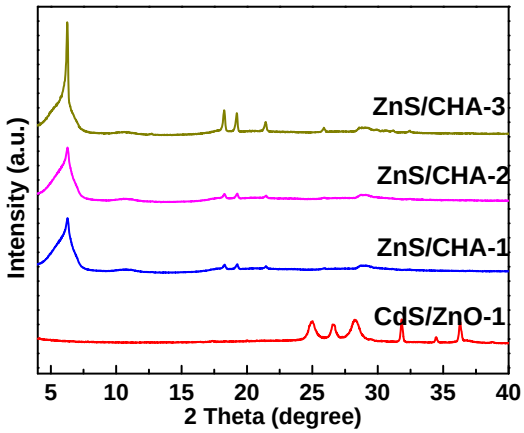

Figure S2. The XRD patterns of ZnS/CHA-1, ZnS/CHA-2, ZnS/CHA-3 and CdS/ZnO-1. The three samples show similar XRD patterns, indicating their similar crystal structures. The biggest feature in the XRD pattern of ZnS/CHA is the presence of a very strong low-angle XRD peak at $2\theta = 6.2$. Similar XRD feature was also observed for some inorganic-organic hybrid materials, [S2] and it was contributed to the formation of mesostructures because of the assembly behavior of the organic amines.

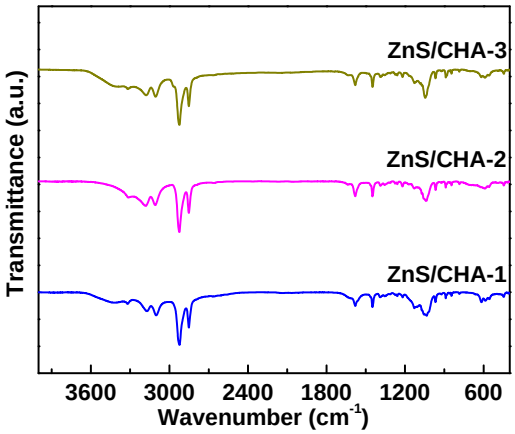

Figure S3. The IR spectra of ZnS/CHA-1, ZnS/CHA-2 and ZnS/CHA-3. The presence of CHA in the ZnS/CHA nanohybrids were confirmed by IR spectroscopy (see figure). The characteristic absorption bands associated with CHA appear in the IR spectrum,[S3] and the stretching vibrations (3175 and 3094 cm^{-1}) and bending vibrations (1588 and 1453 cm^{-1}) of $-NH_2$, the stretching vibrations (2928 and 2855 cm^{-1}) of $-CH_2$, and the stretching vibration C-N (1027 cm^{-1}) are all clearly observed.

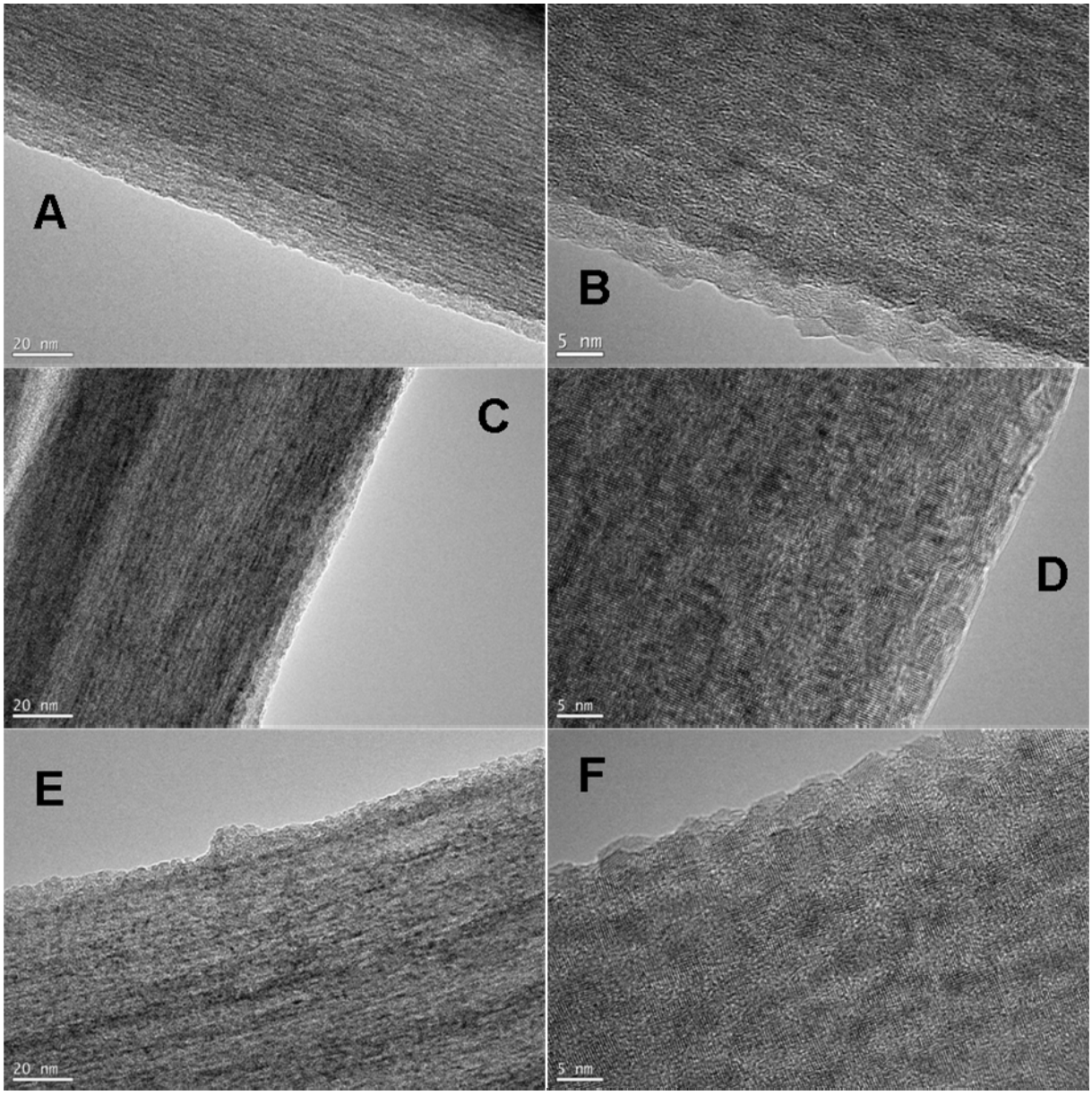

Figure S4. TEM and HRTEM images of (A,B) ZnS/CHA-1, (C,D) ZnS/CHA-2 and (E,F) ZnS/CHA-3.

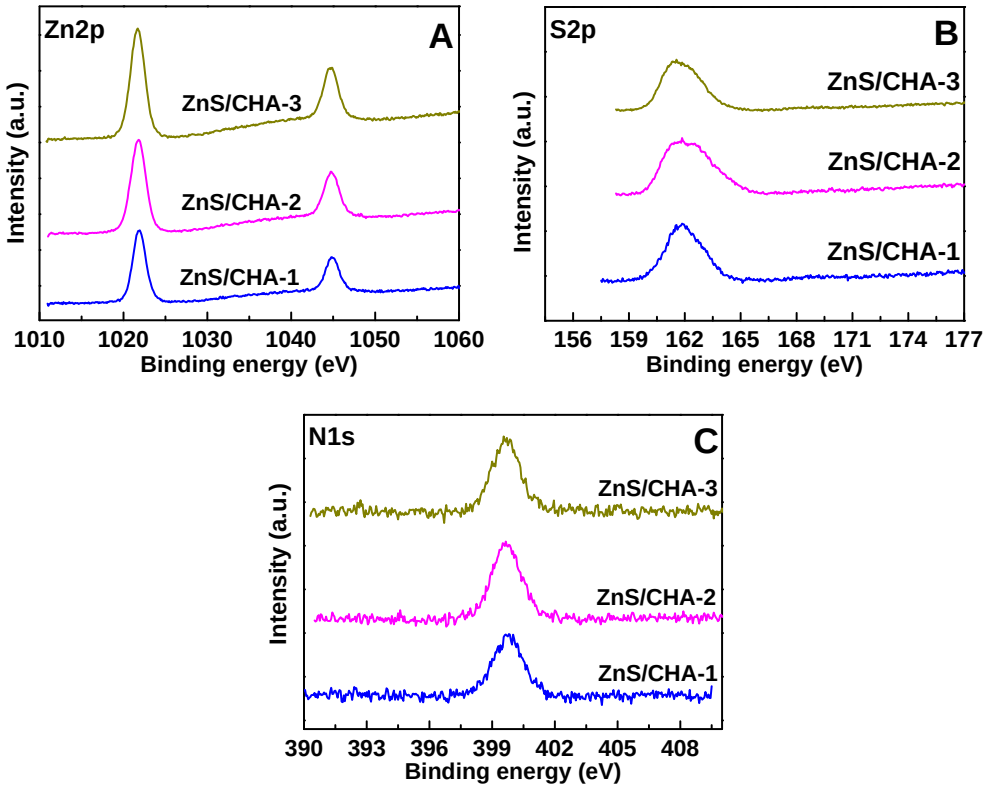

Figure S5. High-resolution XPS spectra of (A) Zn2p, (B) S2p, and (C) N1s for the ZnS/CHA nanohybrids. The spectrum for Zn2p exhibits two peaks at 1021.6 and 1044.7 eV, which are assigned to the 2p3/2 and 2p1/2 core levels of Zn^{2+} in ZnS,[S4] respectively. The spectrum for S2p shows a single peak at 161.8 eV attributable to S^{2-} in ZnS.[S4] The spectrum for N1s also shows a single peak at 399.4 eV, which is close to that for alkylamine (399.6 eV).[S3b] This observation suggests that the CHA molecules in the ZnS/CHA nanohybrids are not protonated, in agreement with the IR spectra.

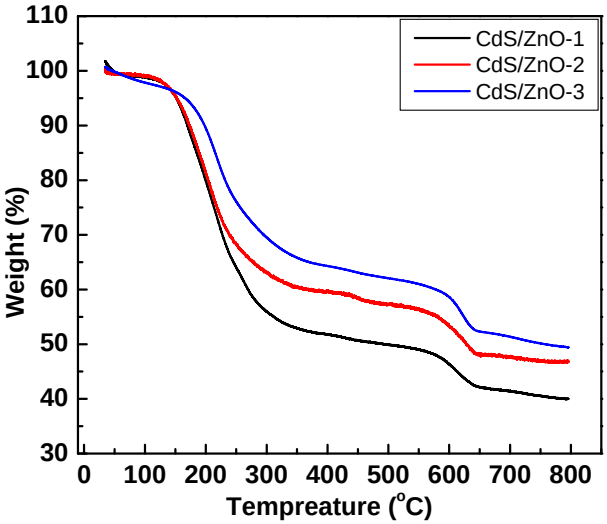

Figure S6. TGA curves in air for the ZnS/CHA nanohybrid materials. As shown in the figure, the weight losses for all the ZnS/CHA nanohybrids occured in a wide temperature mainly range from 150 to 650 °C. The weight loss is attributed to the decomposition of CHA and the oxidation of ZnS nanoparticles to ZnO in the hybrid material. From the weight loss value, the empirical composition of the ZnS/CHA-1, ZnS/CHA-2 and ZnS/CHA-3 was determined to be close to (ZnS)(CHA), $(ZnS)(CHA)_{0.8}$ and $(ZnS)(CHA)_{0.75}$, respectively.

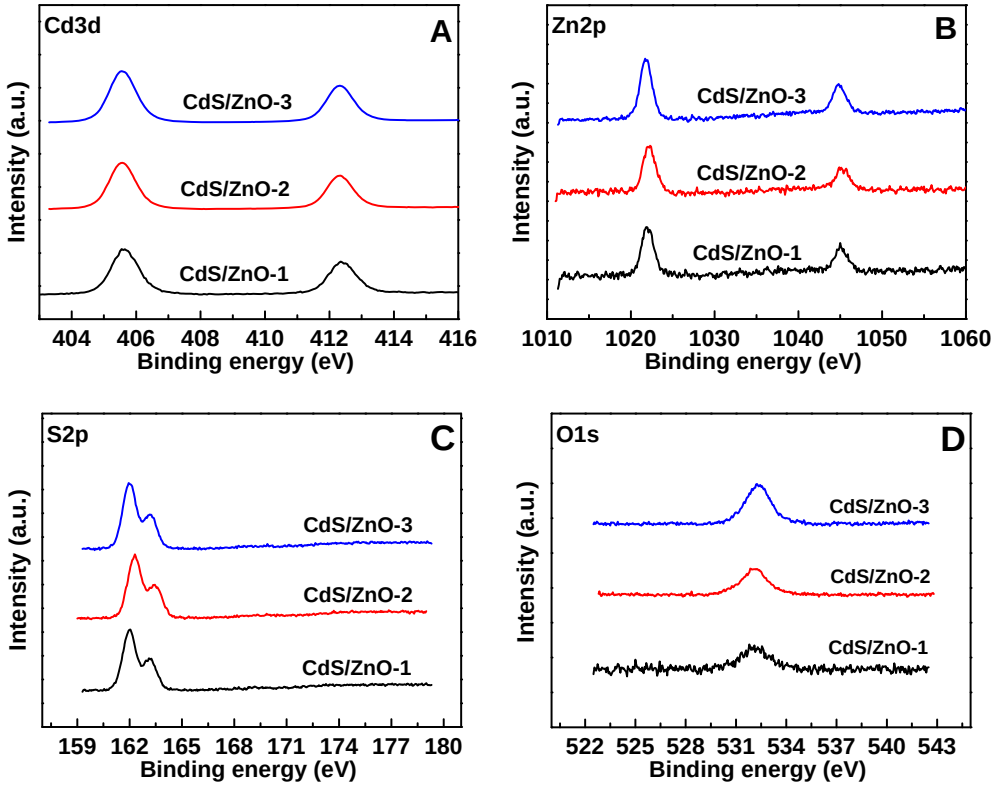

Figure S7. High-resolution XPS spectra of (A) Cd3d, (B) Zn2p, (C) S2p, and (D) O1s for the CdS/ZnO nanocomposite materials.

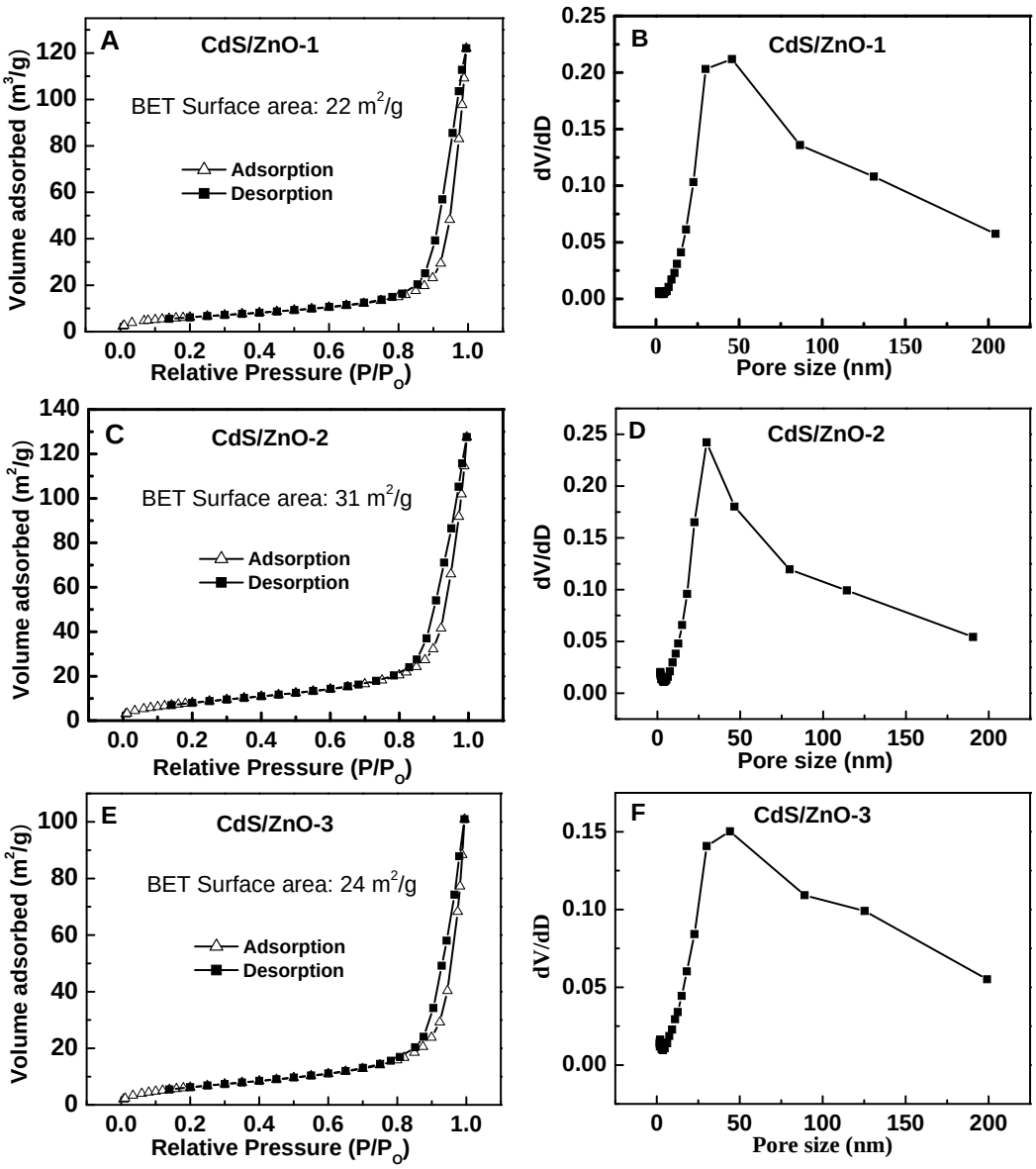

Figure S8. N_2 adsorption/desorption isotherms and the corresponding pore size distribution for (A, B) CdS/ZnO-1, (C, D) CdS/ZnO-2 and (E, F) CdS/ZnO-3. The N_2 adsorption-desorption curves of CdS/ZnO-1, CdS/ZnO-2 and CdS/ZnO-3 exhibit typical type-IV isotherms with an H3 hysteresis loop, indicating the presence of mesoporous/macroporous structure in the materials. The corresponding BJH pore-size distributions derived from adsorption branch of the isotherm show wide pore-size distributions with an average size of ~50 nm, further confirming the existence of mesopores and macropores in the materials. This result is also in agreement with the results obtained with TEM images. The BET surface areas of CdS/ZnO-1, CdS/ZnO-2 and CdS/ZnO-3 were calculated to be 22, 31 and 24 m^2/g, respectively.

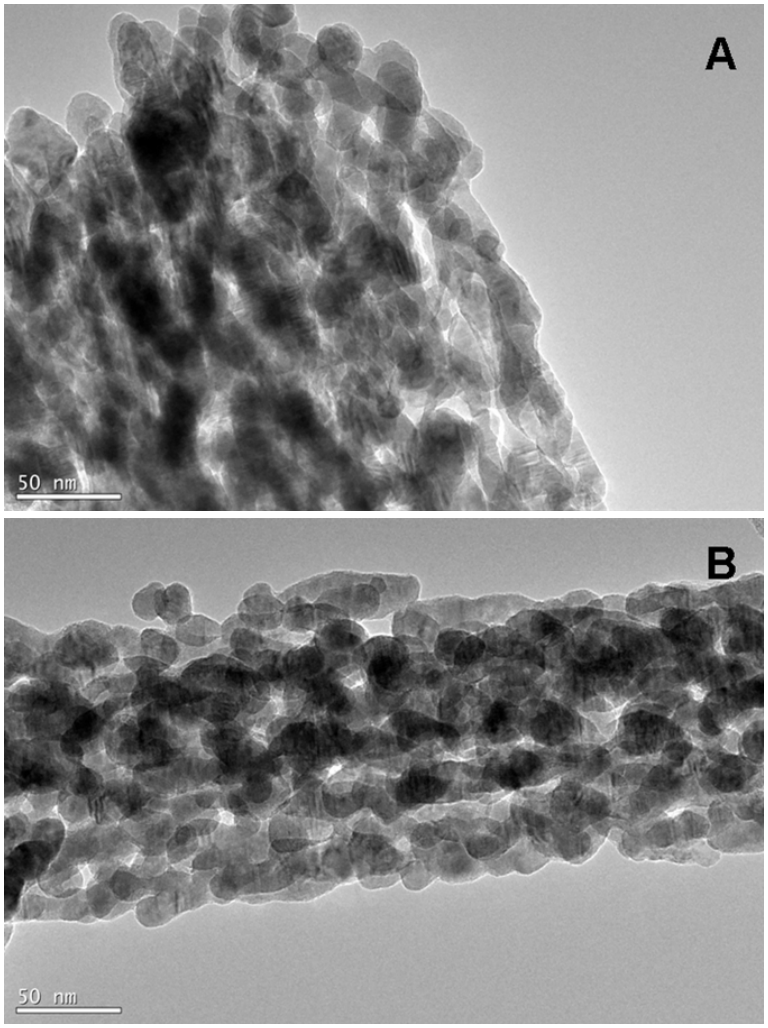

Figure S9. TEM images of (A) CdS/ZnO-1 and (B) CdS/ZnO-2.

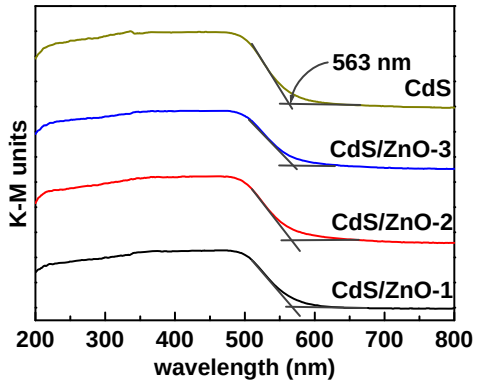

Figure S10. UV/Vis diffuse reflectance spectra of CdS/ZnO-1, CdS/ZnO-2, CdS/ZnO-3 and pure CdS.

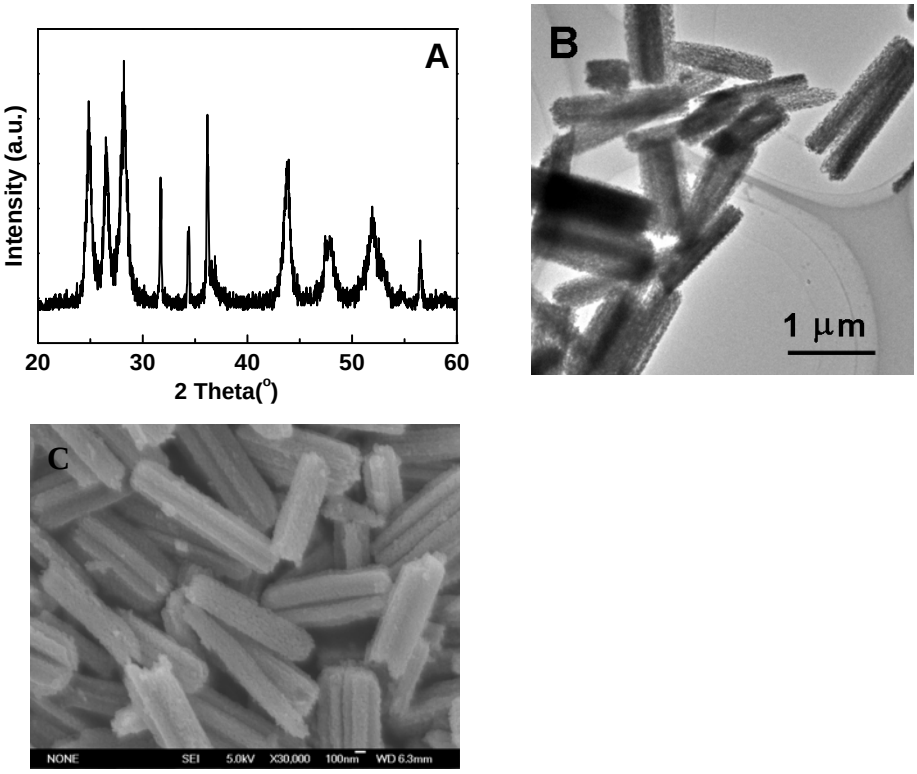

Figure S11. (A) XRD pattern (B) TEM image and (C) SEM image of CdS/ZnO-1 after photocatalytic reaction.

References for ESI Section

[S1] J. Su, X.-X. Zou, G.-D. Li, X. Wei, C. Yan, Y.-N. Wang, J. Zhao, L.-J. Zhou, J.-S. Chen, *J. Phys. Chem. C* **2011**, *115*, 8064.

[S2] (a) M.-R. Gao, W.-T. Yao, H.-B. Yao, S.-H. Yu, *J. Am. Chem. Soc.* **2009**, *131*, 7486; (b) Z.-A. Zang, H.-B. Yao, Y.-X. Zhou, W.-T. Yao, S.-H. Yu, *Chem. Mater.* **2008**, *20*, 4749; (c) W. Yao, S.-H. Yu, X. Huang, J. Jiang, L. Q. Zhao, L. Pan and J. Li, *Adv. Mater.* **2005**, *17*, 2799; (d) L. Fan, H. Song, H. Zhao, G. Pan, H. Yu, X. Bai, S. Li, Y. Lei, Q. Dai, R. Qin, T. Wang, B. Dong, Z. Zheng and X. Ren, *J. Phys. Chem. B* **2006**, *110*, 12948; (e) X.-X. Zou, G.-D. Li, J. Zhao, P.-P. Wang, Y.-N. Wang, L.-J. Zhou, J. Su, L. Li, J.-S. Chen, *Inorg. Chem.* ***2011***, *50*, 9106.

[S3] (a) J. Liu, Z. Guo, F. Meng, T. Luo, M. Li, J. Liu, *Nanotechnology* **2009**, *20*, 125501; (b) Q. Gao, P. Chen, Y. Zhang, Y. Tang, *Adv. Mater.* **2008**, *20*, 1837.